

Contents lists available at [ScienceDirect](https://www.sciencedirect.com)

Journal of Computational and Applied Mathematics

journal homepage: www.elsevier.com/locate/cam

Conditioning and error analysis of nonlocal operators with local boundary conditions

Burak Aksoylu ^{a,b,*}, Adem Kaya ^c^a U.S. Army Research Laboratory, Attn:RDRL-WMM-B, Aberdeen Proving Ground, MD 21005, USA^b Wayne State University, Department of Mathematics, Detroit, MI 48202, USA^c Izmir Institute of Technology, Department of Mathematics, Gulbahce, 35430 Izmir, Turkey

ARTICLE INFO

Article history:
Received 4 June 2017

MSC:
65F35
47G10
74B99

Keywords:
Condition number
Error analysis
Integral operator
Peridynamics
Nonlocal diffusion
Preconditioning

ABSTRACT

We study the conditioning and error analysis of novel nonlocal operators in 1D with local boundary conditions. These operators are used, for instance, in peridynamics (PD) and nonlocal diffusion. The original PD operator uses nonlocal boundary conditions (BC) and nonlocal diffusion. The novel operators agree with the original PD operator in the bulk of the domain and simultaneously enforce local periodic, antiperiodic, Neumann, or Dirichlet BC. We prove sharp bounds for their condition numbers in the parameter δ only, the size of nonlocality. We accomplish sharpness both rigorously and numerically. We also present an error analysis in which we use the Nyström method with the trapezoidal rule for discretization. Using the sharp bounds, we prove that the error bound scales like $\mathcal{O}(h^2\delta^{-2})$ and verify the bound numerically.

The conditioning analysis of the original PD operator was studied by Aksoylu and Unlu (2014). For that operator, we had to resort to a discretized form because we did not have access to the eigenvalues of the analytic operator. Due to analytical construction, we now have direct access to the explicit expression of the eigenvalues of the novel operators in terms of δ . This gives us a big advantage in finding sharp bounds for the condition number without going to a discretized form and makes our analysis easily accessible. We prove that the novel operators have ill-conditioning indicated by δ^{-2} sharp bounds. For the original PD operator, we had proved the similar δ^{-2} ill-conditioning when the mesh size approaches 0. From the conditioning perspective, we conclude that the modification made to the original PD operator to obtain the novel operators that accommodate local BC is minor. Furthermore, the sharp δ^{-2} bounds shed light on the role of δ in nonlocal problems.

© 2017 Elsevier B.V. All rights reserved.

1. Introduction

The integral operators under consideration are used, for instance, in peridynamics (PD), a nonlocal extension of continuum mechanics developed by Silling [1], and nonlocal diffusion [2,3]. The important parameter in these nonlocal formulations is the horizon δ which represents the size of nonlocality. Rather than using a discretized form of the governing operator, it is ideal to directly work with the analytic operator and prove sharp bounds for the condition number of the governing operator in δ only. We accomplish this task in this paper because our construction allows us to write explicitly the expression of the spectrum of the analytic operator.

* Corresponding author at: U.S. Army Research Laboratory, Attn:RDRL-WMM-B, Aberdeen Proving Ground, MD 21005, USA.
E-mail addresses: burak@wayne.edu (B. Aksoylu), ademkaya@iyte.edu.tr (A. Kaya).

We consider problems in 1D and, for simplicity, choose the domain $\Omega := [-1, 1]$. We prefer to use a closed domain in order to properly define an extension of a function as given in (1.3) and (2.1). The original bond based PD governing operator is given as

$$\mathcal{L}_{\text{orig}}u(x) := \int_{\Omega} \widehat{C}(x' - x)u(x)dx' - \int_{\Omega} \widehat{C}(x' - x)u(x')dx', \quad x \in \Omega. \quad (1.1)$$

The existing nonlocal operators in the literature related to nonlocal diffusion [3,4] as well as the operator $\mathcal{L}_{\text{orig}}$ use nonlocal boundary conditions (BC) [1, p. 201]. The first conditioning results of the operator $\mathcal{L}_{\text{orig}}$ were reported in [3,5–7]. We improved these results by revealing sharp bounds in [8].

Our approach to nonlocal problems is fundamentally different because we exclusively want to use local BC. Our major result was the finding that the governing operator of PD equation in \mathbb{R} and nonlocal diffusion in \mathbb{R}^d are functions of the Laplace operator [9]. This result opened the path to the introduction of local BC into the PD theory. We studied local BC in nonlocal problems from various aspects [9–15]. Building on [9], we generalized the results in \mathbb{R} to bounded domains [10,11], a critical feature for all practical applications. In [11], we laid the theoretical foundations and in [10], we applied the foundations to prominent BC such as Dirichlet and Neumann, as well as presented numerical implementation of the corresponding wave propagation. In [13], we constructed novel operators in 1D that agree with the original bond-based PD operator in the bulk of the domain and simultaneously enforce local Neumann and Dirichlet BC which we denote by \mathcal{M}_{N} and \mathcal{M}_{D} , respectively. The design philosophy of the novel operators is to enforce local BC by an appropriate choice of kernel functions. Since the operators encode the BC directly through the kernel, the BC are automatically enforced. That way, we think that we are able to avoid altogether any BC related issues. For surface effects seen in PD, see [16, Chap. 4, 5, 7, and 12] and [17,18]. Furthermore, our approach will provide us the capability to solve important elasticity problems that require local BC such as contact, shear, and traction. In [14], we extended the construction in 1D to arbitrary dimension. We carried out numerical experiments by utilizing \mathcal{M}_{N} and \mathcal{M}_{D} as governing operators in [10]. In [12], we studied other related governing operators. In [15], we give an overview of local BC in general nonlocal problems.

In order to accommodate local BC, we slightly modified the original PD operator $\mathcal{L}_{\text{orig}}$ and defined the operator that is closely related to it by [13]

$$\mathcal{L}u(x) := cu(x) - \int_{\Omega} \widehat{C}(x' - x)u(x')dx', \quad x \in \Omega, \quad (1.2)$$

where $c = \int_{\Omega} C(x')dx'$. For $x, x' \in [-1, 1]$, it follows that $x' - x \in [-2, 2]$. Hence, in (1.2), the kernel function $C(x)$ needs to be extended from Ω to the domain of $\widehat{C}(x' - x)$, which is $\widehat{\Omega} := [-2, 2]$. The default extension is the zero extension defined by

$$\widehat{C}(x) := \begin{cases} 0, & x \in [-2, -1), \\ C(x), & x \in [-1, 1], \\ 0, & x \in (1, 2]. \end{cases} \quad (1.3)$$

Furthermore, the kernel function $C(x)$ is assumed to be even. Namely,

$$C(-x) = C(x).$$

An important first choice of $C(x)$ is the *canonical* kernel function $\chi_{\delta}(x)$ whose only role is the representation of the nonlocal neighborhood, called the *horizon*, by a characteristic function. More precisely, for $x \in \Omega$,

$$\chi_{\delta}(x) := \begin{cases} 1, & x \in (-\delta, \delta) \\ 0, & \text{otherwise.} \end{cases} \quad (1.4)$$

Since the size of nonlocality is determined by δ , the choice of Ω implies that $\delta < 1$, which we assume throughout the paper.

We proved that the operators $\mathcal{L}_{\text{orig}}$ and \mathcal{L} agree in the bulk [13]. The operator \mathcal{L} is based on the generalized convolution operator given in [10,11]. The spectral information of the generalized convolution operator is readily available due to analytical construction. We have direct access to the explicit expression of the eigenvalues in terms of δ . This gives us a big advantage in finding sharp bounds for the condition number. In our previous work [8] which addressed the conditioning of the governing operator in (1.1), we did not have access to the eigenvalues of the analytic operator $\mathcal{L}_{\text{orig}}$. Instead, we had to resort to a discretization of $\mathcal{L}_{\text{orig}}$ in order to obtain sharp bounds for the condition number. Hence, this work presents an approach to obtain sharp bounds different from the one exploited in [8] and our analysis is easily accessible.

Our ultimate goal is to prove an upper and a lower bound of the condition number which contain the same expression of δ . Hence, in our context, *sharpness means that the bounds have the same δ -quantification and the associated constants have no dependence on δ .*

Our construction for the novel operators \mathcal{M}_{N} and \mathcal{M}_{D} is straightforward and easily accessible. The main ingredients are antiperiodic and periodic extensions of kernel functions together with even and odd parts of functions. We also study the governing operators \mathcal{M}_{p} and \mathcal{M}_{a} that enforce local periodic and antiperiodic BC, respectively. Eventually, we will compare the condition number bounds reported in [8] obtained for $\mathcal{L}_{\text{orig}}$ to those we obtain for the aforementioned novel operators.

The main conditioning results of this paper are as follows.

Theorem 1.1. For the governing operators $\mathcal{M}_p, \mathcal{M}_a, \mathcal{M}_N,$ and \mathcal{M}_D given in (2.2), (2.3), (4.2), and (4.3), respectively, the following condition number bounds hold.

$$\begin{aligned} \frac{6}{\pi^2} \delta^{-2} < \kappa_e(\mathcal{M}_p) &< \frac{24}{\pi^2} \delta^{-2}, \\ \frac{24}{\pi^2} \delta^{-2} < \kappa(\mathcal{M}_a), \kappa_e(\mathcal{M}_N), \kappa(\mathcal{M}_D) &< \frac{96}{\pi^2} \delta^{-2}. \end{aligned}$$

Furthermore, the error analysis gives the following bound.

Theorem 1.2. Consider the operator equation

$$\mathcal{M}_{BC} u_{BC} = b_{BC},$$

where $BC = \{a, D\}$. For $h \leq \delta$, let the operators \mathcal{M}_{BC} be discretized by the Nyström method with the trapezoidal rule using $n = 2/h + 1$ quadrature points. For $u, b_{BC} \in C^2(\bar{\Omega})$, any $\delta > 0$, and sufficiently small h , we obtain the following error bound in $L^2(\Omega)$ -norm.

$$\|u - u_n\| = \mathcal{O}(h^2 \delta^{-2}).$$

Our approach is not limited to PD, the abstractness of the theoretical methods used allows generalization to other nonlocal theories. Our approach presents a unique way of combining the powers of abstract operator theory with numerical computing [10]. Similar classes of operators are used in numerous applications such as nonlocal diffusion [2–4], image processing [19], population models, particle systems, phase transition, and coagulation. See the review and news articles [3,20,21] for a comprehensive discussion, and the book [16]. In addition, see the studies dedicated to conditioning analysis, domain decomposition and variational theory [5,6,8], discretization [8,22], and kernel functions [23,24].

The rest of the paper is structured as follows. In Section 2, we define the operators \mathcal{M}_p and \mathcal{M}_a that enforce local periodic and antiperiodic BC, respectively, and present explicit expression of their eigenvalues in terms of δ . In Section 3, first we prove sharp bounds for the operators \mathcal{M}_p and \mathcal{M}_a . In Section 4, we discover that the eigenvalues of the operators \mathcal{M}_N and \mathcal{M}_D are the union of those of \mathcal{M}_p and \mathcal{M}_a . We prove this result by exploiting a commutativity property of the projection operators with the generalized convolutions. In Section 5, in order to numerically verify the condition number bounds obtained from the analytic operator, we employ the Nyström method for discretization. Since all the operators under consideration are self-adjoint, it is reasonable to expect that the discretization produces symmetric matrices. The trapezoidal rule turns out to be ideal for that purpose because it allows us to obtain symmetric matrices by simple algebraic manipulations. In Section 6, we present these algebraic steps as well as the structure of the resulting system matrices. In Section 7, we present an error analysis that involves both the mesh size h and the horizon δ . We verify the error bounds numerically. In Section 8, we report the numerical results regarding the conditioning analysis. In Section 9, we make comparison to the sharp bounds given in [8] for the operator \mathcal{L}_{orig} . We conclude in Section 10.

2. The periodic and antiperiodic operators and their eigenvalues

We define the operators that enforce local periodic, antiperiodic, Neumann, and Dirichlet BC by utilizing the periodic and antiperiodic extensions of $C(x)$ from Ω to $\bar{\Omega}$, respectively, as follows

$$\widehat{C}_p(x) := \begin{cases} C(x+2), & x \in [-2, -1], \\ C(x), & x \in [-1, 1], \\ C(x-2), & x \in (1, 2], \end{cases} \quad \widehat{C}_a(x) := \begin{cases} -C(x+2), & x \in [-2, -1], \\ C(x), & x \in [-1, 1], \\ -C(x-2), & x \in (1, 2]. \end{cases} \tag{2.1}$$

The following operators enforce local periodic and antiperiodic BC, respectively.

$$\mathcal{M}_p u(x) := cu(x) - \int_{\Omega} \widehat{C}_p(x' - x)u(x')dx', \tag{2.2}$$

$$\mathcal{M}_a u(x) := cu(x) - \int_{\Omega} \widehat{C}_a(x' - x)u(x')dx'. \tag{2.3}$$

In order to align with the construction given in [10], we assume that $C(x) \in L^2(\Omega)$, and hence,

$$\widehat{C}(x), \widehat{C}_p(x), \widehat{C}_a(x) \in L^2(\bar{\Omega}). \tag{2.4}$$

Furthermore, we assume that

$$u(x) \in L^2(\Omega) \cap C^1(\partial\Omega). \tag{2.5}$$

The convolution operators in (2.2) and (2.3) in the form of integrals are derived from their (original) series representation. We defined generalized convolution operators in [10,11] in the following series form.

$$\mathcal{C}_{BC} u(x) := \sum_k \langle e_k^{BC} | C \rangle \langle e_k^{BC} | u \rangle e_k^{BC},$$

where $BC = p, a$ and $\langle \cdot | \cdot \rangle$ denotes the inner product in $L^2_C(\Omega)$ and is defined by

$$\langle e_k^{BC} | u \rangle := \int_{\Omega} (e_k^{BC})^*(x') u(x') dx'.$$

In addition, $(e_k^{BC})_k$ is chosen to be a basis associated to a multiple of the Laplace operator with appropriate BC, which we call as the classical operator and denote by Δ_{BC} . The spectrum of Δ_{BC} with classical BC such as periodic, antiperiodic, Neumann, and Dirichlet is purely discrete. Furthermore, we can explicitly calculate the eigenfunctions e_k^{BC} corresponding to each BC. These eigenfunctions form a Hilbert (complete and orthonormal) basis for $L^2_C(\Omega)$ through which the generalized convolution operator is defined. The main reason why we discuss Δ_{BC} is the fact that the governing operator (1.2) turns out to be a function of Δ_{BC} [9–11]. This observation opened a gateway to incorporate local BC to nonlocal theories on bounded domains [11].

In [10], for $u, C \in L^2(\Omega)$, we proved that the operator C_{BC} has the following integral representations.

$$C_p u(x) = \int_{\Omega} \widehat{C}_p(x' - x) u(x') dx', \quad C_a u(x) = \int_{\Omega} \widehat{C}_a(x' - x) u(x') dx'. \quad (2.6)$$

We turn to the series representation to obtain the eigenvalues of the operators \mathcal{M}_p and \mathcal{M}_a . First note that both operators have a purely discrete spectrum consisting of the following eigenvalues

$$\sigma(\Delta_p) = \{k^2 : k \in \mathbb{N}\}, \quad \sigma(\Delta_a) = \{(k + \frac{1}{2})^2 : k \in \mathbb{N}\},$$

with the corresponding normalized eigenfunctions

$$e_k^p(x) := \frac{1}{\sqrt{2}} e^{i\pi k x}, \quad e_k^a(x) := \frac{1}{\sqrt{2}} e^{i\pi(k + \frac{1}{2})x}, \quad k \in \mathbb{N}.$$

Furthermore, the operators \mathcal{M}_p and \mathcal{M}_a are self-adjoint, hence, the condition number calculation reduces to finding

$$\kappa_e(\mathcal{M}_p) = \frac{\lambda_{\max}^p}{\lambda_{\min,2}^p} \quad \text{and} \quad \kappa(\mathcal{M}_a) = \frac{\lambda_{\max}^a}{\lambda_{\min}^a}. \quad (2.7)$$

Throughout the paper, we use the canonical kernel in (1.4), i.e., $C(x) = \chi_{\delta}(x)$. One can easily find the eigenvalues of the operators \mathcal{M}_p and \mathcal{M}_a given, respectively, as follows.

$$\lambda_k^p = 2\delta - \langle e_k^p | C \rangle = \begin{cases} 2\delta - \frac{2 \sin(k\pi\delta)}{k\pi}, & k \in \mathbb{N}^* \\ 0, & k = 0, \end{cases} \quad (2.8)$$

$$\lambda_k^a = 2\delta - \langle e_k^a | C \rangle = 2\delta - \frac{2 \sin((k + \frac{1}{2})\pi\delta)}{(k + \frac{1}{2})\pi}, \quad k \in \mathbb{N}. \quad (2.9)$$

Using continuous extension, we utilize the well-known cardinal sine function defined by

$$\text{sinc}(\theta) := \frac{\sin(\theta)}{\theta}, \quad \theta \geq 0.$$

See Fig. 3.1. The following function is utilized in the expression of eigenvalues of the operators \mathcal{M}_p and \mathcal{M}_a .

$$\lambda(\theta) = 2\delta(1 - \text{sinc}(\theta)). \quad (2.10)$$

Notice that the expressions of λ_k^p and λ_k^a both contain the same function in (2.10), but evaluated at different points:

$$\lambda_k^p = \lambda(\theta_k^p), \quad \lambda_k^a = \lambda(\theta_k^a),$$

where $\theta_k^p = k\pi\delta$, $k \in \mathbb{N}$ and $\theta_k^a = \frac{1}{2}(\pi\delta + 2k\pi\delta)$, $k \in \mathbb{N}$. We immediately see that

$$0 \leq \lambda_k^p, \quad 0 < \lambda_k^a.$$

Furthermore, using basic calculus, it is easy to prove that for $\theta > 0$

$$0 < 1 - \text{sinc}(\theta) < \frac{3}{2}. \quad (2.11)$$

Hence, it is more suitable to work with the expression in (2.10).

3. Sharp bounds for the condition number

3.1. The periodic operator

It is easy to see that λ_{\min}^p occurs when $\text{sinc}(\theta)$ is at its maximum, which occurs when $k = 0$. This leads to $\lambda_{\min}^p = 0$. It means that for the condition number estimate, we have to utilize the effective condition number, which requires the next positive minimum eigenvalue $\lambda_{\min,2}$. We prepare for finding the exact expression of $\lambda_{\min,2}$.

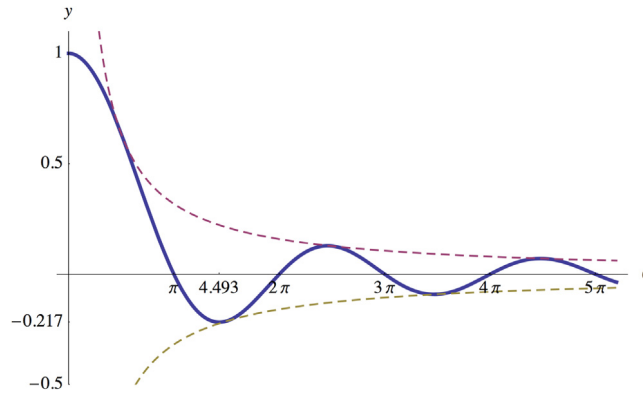


Fig. 3.1. Graph of $\text{sinc}(\theta) = \frac{\sin(\theta)}{\theta}$ (solid line) and $\frac{\pm 1}{\theta}$ (dashed lines).

Lemma 3.1. For $\delta \in (0, 1)$, the following inequality holds.

$$\frac{\sin(k\pi\delta)}{k\pi} < \frac{\sin(\pi\delta)}{\pi}, \quad k = 2, 3, \dots \tag{3.1}$$

Proof. The inequality (3.1) is equivalent to

$$\sin(k\delta\pi) < k \sin(\pi\delta), \quad k = 2, 3, \dots$$

We have two cases. If $\sin(k\pi\delta) \leq \sin(\pi\delta)$, then the proof is straightforward. We consider the case

$$\sin(\pi\delta) < \sin(k\pi\delta). \tag{3.2}$$

We proceed by induction.

• **Induction step 1:** For $k = 2$, we want to prove

$$\sin(2\pi\delta) < 2 \sin(\pi\delta).$$

For that, we define the function

$$f(\delta) := 2 \sin(\pi\delta) - \sin(2\pi\delta),$$

and aim to show that $f(\delta) > 0$. We start by finding the extremal values of f . Note that $f(\delta)$ has only one critical point in the interval $(0, 1)$, i.e., $\delta = \frac{2}{3}$, for which we have $f(\frac{2}{3}) = \frac{3\sqrt{3}}{2}$. After some simple calculation, we obtain that f is monotone increasing and decreasing on $(0, \frac{2}{3})$ and $(\frac{2}{3}, 1)$, respectively. Using the fact $f(0) = f(1) = 0$ and combining the monotonicity information, we obtain $0 < f(\delta) \leq \frac{3\sqrt{3}}{2}$, $\delta \in (0, 1)$, which leads to the desired result.

• **Induction step 2:** We start with the following induction assumption for arbitrary $k > 2$.

$$\sin(k\pi\delta) < k \sin(\pi\delta). \tag{3.3}$$

We aim to show that (3.3) holds for $k + 1$. Using $0 < \sin(\pi\delta)$ and (3.2), we obtain

$$0 < \sin(k\pi\delta). \tag{3.4}$$

Using $\cos(\pi\delta) < 1$ and (3.4), we obtain

$$\cos(\pi\delta) \sin(k\pi\delta) < \sin(k\pi\delta). \tag{3.5}$$

Using (3.5) and the induction assumption (3.3), we arrive at

$$\cos(\pi\delta) \sin(k\pi\delta) < k \sin(\pi\delta). \tag{3.6}$$

Using $\cos(k\pi\delta) \leq 1$, we have

$$\sin(\pi\delta) \cos(k\pi\delta) \leq \sin(\pi\delta). \tag{3.7}$$

Combining (3.6) and (3.7), we arrive at

$$\sin((k + 1)\pi\delta) < (k + 1) \sin(\pi\delta). \quad \square$$

From (2.8), the positive minimum eigenvalue occurs when $k \geq 1$ and by Lemma 3.1, it occurs when $k = 1$. More precisely,

$$\lambda_{\min,2}^p = 2\delta - \frac{2 \sin(\pi \delta)}{\pi}. \tag{3.8}$$

On the other hand, the maximum eigenvalue occurs when $\sin(k\pi \delta) < 0$ for some $k \geq 2$. Using (2.11), we immediately conclude that

$$2\delta < \lambda_{\max}^p < 3\delta. \tag{3.9}$$

In fact, it is possible to find an approximate upper bound smaller than the one given in (3.9). Define

$$\text{sinc}_{\min} := \min_{\theta \geq 0} \text{sinc}(\theta).$$

One can compute that $\text{sinc}_{\min} \approx \text{sinc}(4.493) \approx -0.217$; see Fig. 3.1. Hence, the improved upper bound in (3.9) is approximately 2.434δ . For rigorous treatment, we work with the analytic upper bound in (3.9).

Rather than working with $\lambda_{\min,2}^p$ and λ_{\max}^p , we find it more convenient working directly with the effective condition number $\kappa_e(\mathcal{M}_p)$ given in (2.7) whose bounds are obtained by combining (3.8) and (3.9) as follows.

$$\frac{2\delta}{2\delta - \frac{2 \sin(\pi \delta)}{\pi}} < \kappa_e(\mathcal{M}_p) < \frac{3\delta}{2\delta - \frac{2 \sin(\pi \delta)}{\pi}}. \tag{3.10}$$

We find bounds which have simpler form than the ones given in (3.10)

Lemma 3.2. For $\delta \in (0, 1)$, the following bounds hold.

$$\text{(Periodic-Lower Bound)} \quad \frac{6}{\pi^2} \delta^{-2} < \frac{2\delta}{2\delta - \frac{2 \sin(\pi \delta)}{\pi}} \tag{3.11}$$

$$\text{(Periodic-Upper Bound)} \quad \frac{3\delta}{2\delta - \frac{2 \sin(\pi \delta)}{\pi}} < \frac{24}{\pi^2} \delta^{-2}. \tag{3.12}$$

Proof. See the Appendix. \square

Combining (3.11) and (3.12), finally, we arrive at the sharp condition number bounds of the periodic operator \mathcal{M}_p .

$$\frac{6}{\pi^2} \delta^{-2} < \kappa_e(\mathcal{M}_p) < \frac{24}{\pi^2} \delta^{-2}. \tag{3.13}$$

3.2. The antiperiodic operator

Similar to λ_{\min}^p , λ_{\min}^a occurs when $\text{sinc}(\theta)$ is at its maximum, which occurs when $\theta = (k + \frac{1}{2})\pi \delta$ is closest to 0 for $k \in \mathbb{N}$. Then, we get $k = [\frac{-1}{2}] = 0$. Hence, using (2.9), we obtain

$$\lambda_{\min}^a = 2\delta - \frac{2 \sin(\pi/2 \delta)}{\pi/2}. \tag{3.14}$$

On the other hand, since the eigenvalues λ_k^a sweep the values of the function for λ_k^p in (2.10), the same bounds in (2.11) are also valid for λ_k^a . More precisely,

$$2\delta < \lambda_{\max}^a < 3\delta. \tag{3.15}$$

Similar to (3.10), combining (3.14) and (3.15), we arrive at the following bounds.

$$\frac{2\delta}{2\delta - \frac{2 \sin(\pi/2 \delta)}{\pi/2}} < \kappa(\mathcal{M}_a) < \frac{3\delta}{2\delta - \frac{2 \sin(\pi/2 \delta)}{\pi/2}}. \tag{3.16}$$

We find bounds which have simpler form than the ones given in (3.16)

Lemma 3.3. For $\delta \in (0, 1)$, the following bounds hold.

$$\text{(Antiperiodic-Lower Bound)} \quad \frac{24}{\pi^2} \delta^{-2} < \frac{2\delta}{2\delta - \frac{2 \sin(\pi/2 \delta)}{\pi/2}} \tag{3.17}$$

$$\text{(Antiperiodic-Upper Bound)} \quad \frac{3\delta}{2\delta - \frac{2 \sin(\pi/2 \delta)}{\pi/2}} < \frac{96}{\pi^2} \delta^{-2}. \tag{3.18}$$

Proof. See the [Appendix](#). □

Combining (3.17) and (3.18), finally, we arrive at the sharp condition number bounds of the antiperiodic operator \mathcal{M}_a .

$$\frac{24}{\pi^2} \delta^{-2} < \kappa(\mathcal{M}_a) < \frac{96}{\pi^2} \delta^{-2}. \tag{3.19}$$

4. The Neumann and Dirichlet operators

We constructed the following operators that agree with the original operator $\mathcal{L}_{\text{orig}}$ in the bulk of the domain and simultaneously enforce local homogeneous Dirichlet or Neumann BC [13].

$$\begin{aligned} \mathcal{M}_N u(x) &:= cu(x) - \int_{\Omega} [\widehat{C}_p(x' - x)P_e u(x') + \widehat{C}_a(x' - x)P_o u(x')] dx', \\ \mathcal{M}_D u(x) &:= cu(x) - \int_{\Omega} [\widehat{C}_a(x' - x)P_e u(x') + \widehat{C}_p(x' - x)P_o u(x')] dx', \end{aligned}$$

where we denote the orthogonal projections that give the even and odd parts, respectively, of a function by $P_e, P_o : L^2(\Omega) \rightarrow L^2(\Omega)$, whose definitions are

$$P_e u(x) := \frac{u(x) + u(-x)}{2}, \quad P_o u(x) := \frac{u(x) - u(-x)}{2}.$$

Note that the orthogonal projections have the following properties.

$$P_e^2 = P_e, \quad P_o^2 = P_o, \quad P_e P_o = P_o P_e = 0. \tag{4.1}$$

These properties were also exploited in comparing other related governing operators in [12].

We identify the kernel functions associated to operators \mathcal{M}_N and \mathcal{M}_D utilizing the commutativity property established in [Lemma 4.1](#).

$$(\mathcal{M}_N - c)u(x) = - \int_{\Omega} K_N(x, x')u(x')dx', \tag{4.2}$$

$$(\mathcal{M}_D - c)u(x) = - \int_{\Omega} K_D(x, x')u(x')dx', \tag{4.3}$$

where

$$K_N(x, x') := \frac{1}{2} \{ [\widehat{C}_p(x' - x) + \widehat{C}_p(x' + x)] + [\widehat{C}_a(x' - x) - \widehat{C}_a(x' + x)] \}, \tag{4.4}$$

$$K_D(x, x') := \frac{1}{2} \{ [\widehat{C}_a(x' - x) + \widehat{C}_a(x' + x)] + [\widehat{C}_p(x' - x) - \widehat{C}_p(x' + x)] \}. \tag{4.5}$$

The boundedness of \mathcal{M}_N and \mathcal{M}_D follows from the choice of (2.4) and (2.5). In addition, since \mathcal{M}_N and \mathcal{M}_D are both integral operators, their self-adjointness easily follows from the fact that the corresponding kernels are symmetric (due to evenness of C), i.e., $K_N(x, x') = K_N(x', x)$ and $K_D(x, x') = K_D(x', x)$.

We prove that the operator \mathcal{M}_D enforces homogeneous Dirichlet BC when we assume the same BC on $u(x)$. By the Lebesgue Dominated Convergence Theorem, the limit in the definition of the Dirichlet BC can be interchanged with the integral sign. Now, we check the boundary values by plugging $x = \pm 1$ in (4.5).

$$(\mathcal{M}_D - c)u(\pm 1) = - \int_{\Omega} K_D(\pm 1, x')u(x')dx'. \tag{4.6}$$

Since \widehat{C}_p and \widehat{C}_a are 2-periodic and 2-antiperiodic, respectively, we have

$$\widehat{C}_p(x' \mp 1) = \widehat{C}_p(x' \pm 1) \quad \text{and} \quad \widehat{C}_a(x' \mp 1) = -\widehat{C}_a(x' \pm 1).$$

Hence, the integrand in (4.6) vanishes, i.e., $K_D(\pm 1, x') = 0$. Therefore, we arrive at

$$\mathcal{M}_D u(\pm 1) = cu(\pm 1).$$

When we assume that u satisfies homogeneous Dirichlet BC, i.e., $u(\pm 1) = 0$, we conclude that the operator \mathcal{M}_D enforces homogeneous Dirichlet BC as well.

One can find the proof that the operator \mathcal{M}_N enforces homogeneous Neumann BC in [13]. In order to demonstrate the BC enforcement, we provide some of the numerical experiments in 1D reported in [10]. Galerkin projection method with piecewise polynomials was used for discretization. We solve the following nonlocal wave equation numerically by employing the governing operators \mathcal{M}_N and \mathcal{M}_D .

$$\begin{aligned} u_{tt}(x, t) + \mathcal{M}_{BC}u(x, t) &= 0, \quad (x, t) \in \Omega \times J, \\ u(x, 0) = u_0(x), \quad u_t(x, 0) &= 0, \quad x \in \Omega, \end{aligned}$$

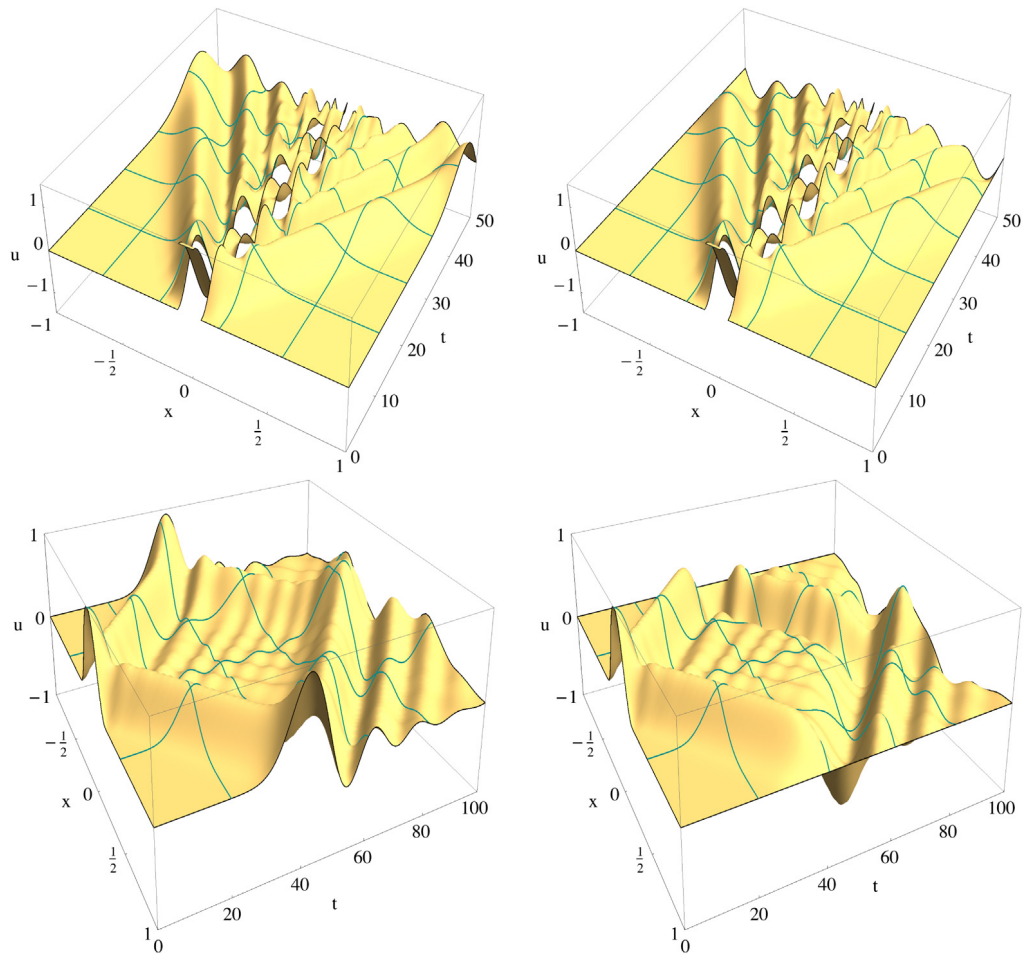


Fig. 4.1. Solution to the nonlocal wave equation with Neumann (left) and Dirichlet (right) BC with discontinuous (top) and continuous (bottom) initial displacement, and vanishing initial velocity. Note that, for all time, BC are satisfied.

where $BC \in \{N, D\}$ and with discontinuous and continuous initial displacement $u_0(x)$. Note that, for all time, BC are satisfied; see Fig. 4.1.

4.1. The spectra of the Neumann and Dirichlet operators and sharp bounds

We can express the operators \mathcal{M}_N and \mathcal{M}_D using the operators C_p and C_a in (2.6) as follows.

$$\begin{aligned} (\mathcal{M}_N - c)u(x) &= -(C_a P_o + C_p P_e)u(x), \\ (\mathcal{M}_D - c)u(x) &= -(C_a P_e + C_p P_o)u(x). \end{aligned}$$

We present a commutativity property that will help us in finding $\sigma(\mathcal{M}_N)$ and $\sigma(\mathcal{M}_D)$.

Lemma 4.1.

$$C_a P_e = P_e C_a, \quad C_a P_o = P_o C_a, \quad C_p P_e = P_e C_p, \quad C_p P_o = P_o C_p. \tag{4.7}$$

Proof. We present the proof for $C_a P_e = P_e C_a$. The other results easily follow. We recall the definition of $C_a u(x)$ in (2.6). We explicitly write $P_e C_a u(x)$. The result follows by a change of variable.

$$\begin{aligned} P_e C_a u(x) &= \frac{1}{2} \left(\int_{\Omega} \widehat{C}_a(x' - x)u(x')dx' + \int_{\Omega} \widehat{C}_a(x' + x)u(x')dx' \right) \\ &= \frac{1}{2} \left(\int_{\Omega} \widehat{C}_a(x' - x)u(x')dx' + \int_{\Omega} \widehat{C}_a(x' - x)u(-x')dx' \right) \end{aligned}$$

$$\begin{aligned} &= \int_{\Omega} \widehat{C}_a(x' - x) P_e u(x') dx' \\ &= C_a P_e u(x). \quad \square \end{aligned}$$

We are now in a position to present the main spectral result for the operators \mathcal{M}_N and \mathcal{M}_D .

Lemma 4.2. *The spectra of the operators \mathcal{M}_N and \mathcal{M}_D are as follows.*

$$\sigma(\mathcal{M}_N) = \sigma(\mathcal{M}_a) \cup \sigma(\mathcal{M}_p) \quad \text{and} \quad \sigma(\mathcal{M}_D) = \sigma(\mathcal{M}_a) \cup \sigma(\mathcal{M}_p) \setminus \{0\}. \tag{4.8}$$

Proof. We present the result for \mathcal{M}_D only. The result for the case of \mathcal{M}_N follows in a similar way. It is obvious that $\sigma(\mathcal{M}_D) = \sigma(\mathcal{M}_D - c) + c$ and is more convenient to work with $\sigma(\mathcal{M}_D - c)$.

• $\sigma(\mathcal{M}_p - c) \cup \sigma(\mathcal{M}_a - c) \subset \sigma(\mathcal{M}_D - c)$:

Let $\lambda^a \in \sigma(\mathcal{M}_a - c)$. Namely, there exists an eigenfunction u^a satisfying $(\mathcal{M}_a - c)u^a = \lambda^a u^a$. Define $v^a := P_e u^a$. Then, using the properties $P_e^2 = P_e$ and $P_o P_e = 0$ given in (4.1), we obtain

$$\begin{aligned} (\mathcal{M}_D - c)v^a &= -(C_a P_e + C_p P_o) P_e u^a \\ &= -C_a P_e u^a = -P_e C_a u^a = P_e (\mathcal{M}_a - c) u^a = \lambda^a P_e u^a = \lambda^a v^a. \end{aligned} \tag{4.9}$$

Hence, $\sigma(\mathcal{M}_a - c) \subset \sigma(\mathcal{M}_D - c)$.

Similarly, let $\lambda^p \in \sigma(\mathcal{M}_p - c)$. Namely, there exists an eigenfunction u^p $(\mathcal{M}_p - c)u^p = \lambda^p u^p$. Define $v^p := P_o u^p$. Note that $0 \in \sigma(\mathcal{M}_p - c) = \sigma(C_p)$ with the corresponding eigenfunction $u^p = 1$. Since $v^p = P_o 1 = 0$, we cannot utilize it as an eigenfunction, hence, the value 0 needs to be excluded. Then, using $P_o^2 = P_o$ and $P_e P_o = 0$, we obtain

$$\begin{aligned} (\mathcal{M}_D - c)v^p &= -(C_a P_e + C_p P_o) P_o u^p \\ &= -C_p P_o u^p = -P_o C_p u^p = P_o (\mathcal{M}_p - c) u^p = \lambda^p P_o u^p = \lambda^p v^p. \end{aligned} \tag{4.10}$$

Hence, $\sigma(\mathcal{M}_p - c) \subset \sigma(\mathcal{M}_D - c)$. Combining (4.9) and (4.10), the result follows.

• $\sigma(\mathcal{M}_D - c) \subset \sigma(\mathcal{M}_p - c) \cup \sigma(\mathcal{M}_a - c)$:

Let $\lambda^D \in \sigma(\mathcal{M}_D - c)$. Namely, $(\mathcal{M}_D - c)u^D = \lambda^D u^D$. Then, decompose u^D as follows:

$$-(C_a P_e + C_p P_o)(P_e + P_o)u^D = \lambda^D (P_e + P_o)u^D.$$

Collecting the terms with P_e and P_o on each side and using commutativity in (4.7), we obtain

$$P_e(-C_a - \lambda^D)u^D + P_o(-C_p - \lambda^D)u^D = 0. \tag{4.11}$$

Since the operators P_e and P_o are orthogonal projections, each term in (4.11) must be equal to the zero function. Hence, we arrive at

$$\begin{aligned} (\mathcal{M}_a - c)P_e u^D &= -C_a P_e u^D = \lambda^D P_e u^D, \\ (\mathcal{M}_p - c)P_o u^D &= -C_p P_o u^D = \lambda^D P_o u^D. \end{aligned}$$

Consequently, $\lambda^D \in \sigma(\mathcal{M}_a - c) \cup \sigma(\mathcal{M}_p - c)$. \square

The condition number of the operators \mathcal{M}_D and \mathcal{M}_N easily follow from the spectral result in (4.8).

Corollary 4.3.

$$\kappa_e(\mathcal{M}_N) = \kappa(\mathcal{M}_D) = \frac{\max\{\lambda_{\max}^p, \lambda_{\max}^a\}}{\min\{\lambda_{\min,2}^p, \lambda_{\min}^a\}}.$$

Recalling the values of $\lambda_{\min,2}^p$ in (3.8) and λ_{\min}^a in (3.14), we immediately see that

$$0 < \lambda_{\min}^a \leq \lambda_{\min,2}^p.$$

Hence, the condition numbers reduce to

$$\kappa_e(\mathcal{M}_N) = \kappa(\mathcal{M}_D) = \frac{\max\{\lambda_{\max}^p, \lambda_{\max}^a\}}{\lambda_{\min}^a}. \tag{4.12}$$

On the other hand, we have the same bounds for λ_{\max}^p and λ_{\max}^a using (3.9) and (3.15), respectively. Consequently, combining this fact with (4.12), the bounds for the condition numbers $\kappa(\mathcal{M}_D)$ and $\kappa_e(\mathcal{M}_N)$ are identical to those of the antiperiodic operator \mathcal{M}_a given in (3.16). Hence, the bounds provided in Lemma 3.3 are valid for $\kappa_e(\mathcal{M}_N)$ and $\kappa(\mathcal{M}_D)$.

5. The discretization and the quadrature rule

We want to verify the condition number bounds numerically. Our governing operator falls into the class of Fredholm integral equations of the second kind. The projection and the Nyström methods are the well-known types of discretization for this class [25, Chap. 12]. We employ the Nyström method. We are dealing with integral equations, so, one has to pay special attention to the quadrature rule. Since the overarching goal of this study is to accommodate local BC, it is essential to use values at boundary nodes in the quadrature rule. The Gaussian quadrature rule is not suitable because it does not use boundary nodes. However, both the trapezoidal and the Simpson rules use boundary nodes, and hence, are plausible for such a task.

Furthermore, since the governing operator is self-adjoint, a discretization that produces symmetric matrices is desirable. Since the Simpson rule is more involved, obtaining symmetric matrices seems more cumbersome than that from the trapezoidal rule. The trapezoidal rule allows us to obtain symmetric matrices by simple algebraic manipulations; see Section 6. Consequently, we employ the trapezoidal rule.

Let us write the definition of periodic and antiperiodic extensions of the kernel function $\chi_\delta(x)$.

$$\hat{\chi}_{\delta,p}(x) := \begin{cases} 1, & x \in [-2, -2 + \delta) \\ 1, & x \in (-\delta, \delta) \\ 1, & x \in (2 - \delta, 2] \\ 0, & \text{otherwise,} \end{cases} \quad \hat{\chi}_{\delta,a}(x) := \begin{cases} -1, & x \in [-2, -2 + \delta) \\ 1, & x \in (-\delta, \delta) \\ -1, & x \in (2 - \delta, 2] \\ 0, & \text{otherwise.} \end{cases}$$

When we state the range of the x' -variable, we have

$$\hat{\chi}_{\delta,p}(x' - x) := \begin{cases} 1, & x' \in [x - 2, x - 2 + \delta) \\ 1, & x' \in (x - \delta, x + \delta) \\ 1, & x' \in (x + 2 - \delta, x + 2] \\ 0, & \text{otherwise,} \end{cases} \quad \hat{\chi}_{\delta,a}(x' - x) := \begin{cases} -1, & x' \in [x - 2, x - 2 + \delta) \\ 1, & x' \in (x - \delta, x + \delta) \\ -1, & x' \in (x + 2 - \delta, x + 2] \\ 0, & \text{otherwise.} \end{cases} \tag{5.1}$$

By explicitly stating the intervals of the x -variable and recalling the fact that $x', x \in \Omega$, we can write (5.1) more explicitly as follows. Also, see [12, Fig. 1].

$$\hat{\chi}_{\delta,p}(x' - x) := \begin{cases} 1, & x \in [-1, -1 + \delta) & x' \in [-1, x + \delta) \\ 1, & x \in [-1, -1 + \delta) & x' \in (x + 2 - \delta, 1] \\ 1, & x \in [-1 + \delta, 1 - \delta] & x' \in (x - \delta, x + \delta) \\ 1, & x \in (1 - \delta, 1] & x' \in [-1, x - 2 + \delta) \\ 1, & x \in (1 - \delta, 1] & x' \in (x - \delta, 1] \\ 0, & \text{otherwise,} \end{cases} \tag{5.2}$$

$$\hat{\chi}_{\delta,a}(x' - x) := \begin{cases} 1, & x \in [-1, -1 + \delta) & x' \in [-1, x + \delta) \\ -1, & x \in [-1, -1 + \delta) & x' \in (x + 2 - \delta, 1] \\ 1, & x \in [-1 + \delta, 1 - \delta] & x' \in (x - \delta, x + \delta) \\ -1, & x \in (1 - \delta, 1] & x' \in [-1, x - 2 + \delta) \\ 1, & x \in (1 - \delta, 1] & x' \in (x - \delta, 1] \\ 0, & \text{otherwise.} \end{cases} \tag{5.3}$$

Using (5.2) and (5.3), we obtain the following piecewise representation of the operators which leads to a more convenient implementation of the trapezoidal rule.

$$(\mathcal{M}_p - c)u(x) := - \begin{cases} \int_{-1}^{x+\delta} u(x')dx' + \int_{x+2-\delta}^1 u(x')dx', & x \in [-1, -1 + \delta), \\ \int_{-1}^{x+\delta} u(x')dx', & x \in [-1 + \delta, 1 - \delta], \\ \int_{-1}^{x-\delta} u(x')dx' + \int_{x-\delta}^1 u(x')dx', & x \in (1 - \delta, 1], \end{cases} \tag{5.4}$$

$$(\mathcal{M}_a - c)u(x) := - \begin{cases} \int_{-1}^{x+\delta} u(x')dx' - \int_{x+2-\delta}^1 u(x')dx', & x \in [-1, -1 + \delta), \\ \int_{-1}^{x+\delta} u(x')dx', & x \in [-1 + \delta, 1 - \delta], \\ - \int_{-1}^{x-2+\delta} u(x')dx' + \int_{x-\delta}^1 u(x')dx', & x \in (1 - \delta, 1]. \end{cases} \tag{5.5}$$

Utilizing (4.4) and (4.5), we also obtain the following.

$$(\mathcal{M}_N - c)u(x) := - \begin{cases} \int_{-1}^{x+\delta} u(x')dx' + \int_{-1}^{-x-2+\delta} u(x')dx', & x \in [-1, -1 + \delta), \\ \int_{x-\delta}^{x+\delta} u(x')dx', & x \in [-1 + \delta, 1 - \delta], \\ \int_{-x+2-\delta}^1 u(x')dx' + \int_{x-\delta}^1 u(x')dx', & x \in (1 - \delta, 1], \end{cases} \tag{5.6}$$

$$(\mathcal{M}_D - c)u(x) := - \begin{cases} \int_{-1}^{x+\delta} u(x')dx' - \int_{-1}^{-x-2+\delta} u(x')dx', & x \in [-1, -1 + \delta), \\ \int_{x-\delta}^{x+\delta} u(x')dx', & x \in [-1 + \delta, 1 - \delta], \\ - \int_{-x+2-\delta}^1 u(x')dx' + \int_{x-\delta}^1 u(x')dx', & x \in (1 - \delta, 1]. \end{cases} \tag{5.7}$$

We discretize the above equations by choosing a uniformly distributed set of points $x_i, i = 1, \dots, N$ in $[-1, 1]$. Then, we apply the trapezoidal rule by setting the set of points x_i as quadrature points in the integrals given in (5.4), (5.5), (5.6), and (5.7). We obtain the following system matrices

$$A_{BC} u_{BC} = b_{BC},$$

where $BC = \{p, a, N, D\}$. Note that the system matrices A_{BC} are not symmetric. Next, we present how to obtain symmetric ones.

6. Obtaining symmetric system matrices and their structure

The governing operator is self-adjoint, hence it is natural to expect the discretization to produce symmetric matrices. Direct application of the trapezoidal rule leads to nonsymmetric matrices. We can rectify the symmetry issue by simple algebraic manipulations. Obtaining symmetric matrices brings an additional advantage. When the matrices are symmetric, the condition number reduces to the ratio of the maximum and minimum eigenvalues. We verify the condition number numerically and report these ratios in Tables 8.1, 8.2, 8.3, and 8.4.

We present an instance of the system matrix for each BC considered. For convenience of comparison, we utilize the same kernel function $C(x) = \chi_\delta(x)$ given in (1.4) with $\delta = \frac{1}{2}$. Throughout the paper, we assume that $h \leq \delta$. In order to demonstrate the algebraic operations needed to obtain a symmetric matrix, we choose $h = \frac{1}{2}$ so that we have small sized system matrices. We start with the periodic BC and see that the corresponding system matrix is not symmetric as seen in the following.

$$A_p = \begin{bmatrix} c - \frac{h}{2} & -\frac{h}{2} & 0 & -\frac{h}{2} & -\frac{h}{2} \\ -\frac{h}{2} & c - h & -\frac{h}{2} & 0 & 0 \\ 0 & -\frac{h}{2} & c - h & -\frac{h}{2} & 0 \\ 0 & 0 & -\frac{h}{2} & c - h & -\frac{h}{2} \\ -\frac{h}{2} & -\frac{h}{2} & 0 & -\frac{h}{2} & c - \frac{h}{2} \end{bmatrix}_{5 \times 5}.$$

We can easily obtain a symmetric matrix by applying the BC to the system equations. Namely, by setting $(u_p)_1 = (u_p)_N$ and $(b_p)_1 = (b_p)_N$. When we add the last column to the first one, we see that the first and last rows are identical. Using $(b_p)_1 = (b_p)_N$, we can eliminate the last row because it is identical to the first row. This gives rise to a reduced system matrix of size $(N - 1) \times (N - 1)$ and the resulting matrix is symmetric.

For the antiperiodic BC, we obtain the following system matrix.

$$A_a = \begin{bmatrix} c - \frac{h}{2} & -\frac{h}{2} & 0 & \frac{h}{2} & \frac{h}{2} \\ -\frac{h}{2} & c - h & -\frac{h}{2} & 0 & 0 \\ 0 & -\frac{h}{2} & c - h & -\frac{h}{2} & 0 \\ 0 & 0 & -\frac{h}{2} & c - h & -\frac{h}{2} \\ \frac{h}{2} & \frac{h}{2} & 0 & -\frac{h}{2} & c - \frac{h}{2} \end{bmatrix}_{5 \times 5}.$$

$$r_p = [c - h, \overbrace{-h, \dots, -h}^{\frac{\delta}{h} - 1}, \frac{-h}{2}, 0, \dots, 0, \frac{-h}{2}, \overbrace{-h, \dots, -h}^{\frac{\delta}{h} - 1}]$$

Fig. 6.1. The first row of the matrix A_p^s .

$$r_a = [c - h, \overbrace{-h, \dots, -h}^{\frac{\delta}{h} - 1}, \frac{-h}{2}, 0, \dots, 0, \frac{h}{2}, \overbrace{h, \dots, h}^{\frac{\delta}{h} - 1}]$$

Fig. 6.2. The first row of the matrix A_a^s .

Similar to the periodic BC case, we can obtain a symmetric matrix by applying the BC to the system equations. Namely, by setting $(u_a)_1 = -(u_a)_N$ and $(b_a)_1 = -(b_a)_N$. When we subtract the last column from the first one, we see that the first and last rows are identical. Using $(b_a)_1 = -(b_a)_N$, we can eliminate the last row because it is identical to the first one. This gives rise to a reduced system matrix of size $(N - 1) \times (N - 1)$ and the resulting matrix is symmetric.

For the Neumann BC, we obtain the following system matrix.

$$A_N = \begin{bmatrix} c - h & -h & 0 & 0 & 0 \\ -\frac{h}{2} & c - h & -\frac{h}{2} & 0 & 0 \\ 0 & -\frac{h}{2} & c - h & -\frac{h}{2} & 0 \\ 0 & 0 & -\frac{h}{2} & c - h & -\frac{h}{2} \\ 0 & 0 & 0 & -h & c - h \end{bmatrix}_{5 \times 5}.$$

We multiply the first and last rows by 1/2 as well as the entries $(b_N)_1$ and $(b_N)_N$. This multiplication operation gives an equivalent system matrix which is symmetric.

For the Dirichlet BC, we obtain the following system matrix.

$$A_D = \begin{bmatrix} c & 0 & 0 & 0 & 0 \\ -\frac{h}{2} & c - h & -\frac{h}{2} & 0 & 0 \\ 0 & -\frac{h}{2} & c - h & -\frac{h}{2} & 0 \\ 0 & 0 & -\frac{h}{2} & c - h & -\frac{h}{2} \\ 0 & 0 & 0 & 0 & c \end{bmatrix}_{5 \times 5}.$$

The values $(u_D)_1$ and $(u_D)_N$ are known because they are part of the BC. Hence, by deleting the first and last columns as well as the first and last rows, we obtain a symmetric system matrix of size $(N - 2) \times (N - 2)$.

We present the structure of the system matrices. The matrix A_p^s is symmetric positive semidefinite, whereas the matrix A_a^s is symmetric positive definite. Both matrices are of size $(N - 1) \times (N - 1)$, diagonally dominant, and Toeplitz. For the matrix definition, it is sufficient to provide only the first row due to the Toeplitz property. Assuming $h \leq \delta$, we present the first rows of A_p^s and A_a^s in Figs. 6.2 and 6.1, respectively.

The matrix A_N^s is symmetric positive semidefinite and is of size $N \times N$. Whereas the matrix A_D^s is symmetric positive definite and is of size $(N - 2) \times (N - 2)$. Both matrices are diagonally dominant. Assuming $h \leq \delta$, we present the matrix $A_N^s - cI$ in Fig. 6.3 and assuming $2h \leq \delta$, we present the matrix $A_D^s - cI$ in Fig. 6.4. In addition, both A_p^s and A_N^s have the zero row sum property.

7. Error analysis

For error analysis, we define a new integral operator by rewriting the operator expressions in (5.4), (5.5), (5.6), and (5.7) in the form

$$\mathcal{T}_{BC}u := (\mathcal{M}_{BC} - c)u,$$

where $BC = \{p, a, N, D\}$. The explicit expression of \mathcal{T}_{BC} is

$$\mathcal{T}_{BC}u(x) = - \int_{\Omega} K_{BC}(x, x')u(x')dx'.$$

$$A_{\mathbb{N}}^s - cI = \begin{bmatrix} \frac{-c-h}{2} & \overbrace{-h \cdots -h}^{\frac{\delta}{h}-1} & \frac{-h}{2} & 0 & \cdots & 0 \\ -h & -2h & \cdots & -2h & \frac{-5h}{2} & -h & \cdots & \vdots \\ \vdots & \vdots & \ddots & \ddots & \ddots & \ddots & \ddots & 0 \\ -h & -2h & \ddots & \ddots & \cdots & \cdots & -h & \frac{-h}{2} \\ -h & \frac{-5h}{2} & \ddots & \cdots & \cdots & \cdots & \frac{-5h}{2} & -h \\ \frac{-h}{2} & -h & \cdots & \cdots & \ddots & \ddots & -2h & -h \\ 0 & \ddots & \ddots & \cdots & \ddots & \ddots & \vdots & \vdots \\ \vdots & \ddots & \ddots & -h & \frac{-5h}{2} & -2h & \cdots & -2h & -h \\ 0 & \cdots & 0 & \frac{-h}{2} & -h & -h & \cdots & -h & \frac{-c-h}{2} \end{bmatrix} \left. \vphantom{\begin{bmatrix} \end{bmatrix}} \right\} \frac{\delta}{h} - 1$$

Fig. 6.3. Structure of the matrix $A_{\mathbb{N}}^s - cI$.

$$A_{\mathbb{D}}^s - cI = \begin{bmatrix} 0 & \cdots & 0 & \frac{-h}{2} & -h & \frac{-h}{2} & 0 & \cdots & 0 \\ \vdots & \ddots & \ddots & \ddots & \ddots & \ddots & \ddots & \ddots & \vdots \\ 0 & \ddots & \ddots & \cdots & \cdots & \ddots & \ddots & \ddots & 0 \\ \frac{-h}{2} & \ddots & \cdots & \cdots & \cdots & \cdots & \ddots & \ddots & \frac{-h}{2} \\ -h & \cdots & \cdots & \cdots & \cdots & \cdots & \cdots & \cdots & -h \\ \frac{-h}{2} & \ddots & \cdots & \cdots & \cdots & \cdots & \ddots & \ddots & \frac{-h}{2} \\ 0 & \ddots & \ddots & \cdots & \cdots & \cdots & \ddots & \ddots & 0 \\ \vdots & \ddots & \ddots & \ddots & \cdots & \ddots & \ddots & \ddots & \vdots \\ 0 & \cdots & 0 & \frac{-h}{2} & -h & \frac{-h}{2} & 0 & \cdots & 0 \end{bmatrix} \left. \vphantom{\begin{bmatrix} \end{bmatrix}} \right\} \frac{\delta}{h} - 2$$

Fig. 6.4. Structure of the matrix $A_{\mathbb{D}}^s - cI$.

Since error analysis calls for differentiation, we assume that $u, b \in C^2(\overline{\Omega})$. Furthermore, our analysis assumes invertible operators. Since the spectra of the operators \mathcal{M}_p and \mathcal{M}_N contain zero eigenvalues, the error analysis we carry out covers the operators \mathcal{M}_a and \mathcal{M}_D . The exact expressions of \mathcal{T}_a and \mathcal{T}_D can be obtained from (2.3) and (4.5), respectively.

The operators \mathcal{T}_p and \mathcal{T}_a are self-adjoint and compact. Since the operators \mathcal{T}_N and \mathcal{T}_D are linear combinations of \mathcal{T}_p and \mathcal{T}_a , they are also self-adjoint and compact. We prefer to work with the scaled operators given in the following.

$$\overline{\mathcal{M}}_{BC}u = (I - \overline{\mathcal{T}}_{BC})u = \overline{b},$$

where I is the identity operator, $\overline{\mathcal{T}}_{BC} := \frac{1}{c}\mathcal{T}_{BC}$, and $\overline{b} := \frac{1}{c}b$ for $BC = \{a, D\}$. From (3.14), we have

$$\|\overline{\mathcal{T}}_a\| = \frac{\sin(\pi\delta/2)}{\pi\delta/2}.$$

On the other hand, from (4.8), we also have

$$\|\overline{\mathcal{T}}_D\| = \frac{\sin(\pi\delta/2)}{\pi\delta/2}.$$

Consequently, for $BC = \{a, D\}$, we have

$$\|\overline{\mathcal{T}}_{BC}\| < 1,$$

which indicates that the operators $\overline{\mathcal{T}}_{BC}$ are contractions. We can conclude that the operator $I - \overline{\mathcal{T}}_{BC}$ is invertible. It is well known that

$$\|(I - \overline{\mathcal{T}}_{BC})^{-1}\| \leq \frac{1}{1 - \|\overline{\mathcal{T}}_{BC}\|}. \tag{7.1}$$

From (3.18), we have

$$\frac{1}{1 - \frac{\sin(\delta\pi/2)}{\delta\pi/2}} < \frac{64}{\pi^2} \delta^{-2}. \tag{7.2}$$

Hence, combining (7.1) and (7.2), we arrive at

$$\|(I - \overline{\mathcal{T}}_{BC})^{-1}\| \leq \frac{64}{\pi^2} \delta^{-2}. \tag{7.3}$$

7.1. Bounds for the error

Let us define the sequence of operators

$$\overline{\mathcal{T}}_{BC}^n u(x) := - \sum_{i=1}^n \alpha_i K_{BC}(x_i, x) u(x_i),$$

where α_i denotes the quadrature weight. The operators $\overline{\mathcal{T}}_{BC}$ are compact. Since the trapezoidal rule is convergent, the sequence $\overline{\mathcal{T}}_{BC}^n$ is collectively compact and pointwise convergent, i.e., $\overline{\mathcal{T}}_{BC}^n u \rightarrow \overline{\mathcal{T}}_{BC} u$. A bound for the error can be obtained in the following fashion; see [26, Thm.10.8]. For sufficiently large n , more precisely, for all n with

$$\|(I - \overline{\mathcal{T}}_{BC})^{-1}(\overline{\mathcal{T}}_{BC}^n - \overline{\mathcal{T}}_{BC})\overline{\mathcal{T}}_{BC}^n\| < 1,$$

the solutions to the equations

$$u - \overline{\mathcal{T}}_{BC} u = \bar{b}, \quad u_n - \overline{\mathcal{T}}_{BC}^n u_n = \bar{b}$$

satisfy the following error bound.

$$\|u - u_n\| \leq \|(I - \overline{\mathcal{T}}_{BC})^{-1}\| \frac{\|(\overline{\mathcal{T}}_{BC}^n - \overline{\mathcal{T}}_{BC})\bar{b}\| + \|(\overline{\mathcal{T}}_{BC}^n - \overline{\mathcal{T}}_{BC})\overline{\mathcal{T}}_{BC}^n u\|}{1 - \|(I - \overline{\mathcal{T}}_{BC})^{-1}(\overline{\mathcal{T}}_{BC}^n - \overline{\mathcal{T}}_{BC})\overline{\mathcal{T}}_{BC}^n\|}. \tag{7.4}$$

A bound for the term $\|(\overline{\mathcal{T}}_{BC}^n - \overline{\mathcal{T}}_{BC})\overline{\mathcal{T}}_{BC}^n\|$ can be given as follows [27, (4.1.21)].

$$\|(\overline{\mathcal{T}}_{BC}^n - \overline{\mathcal{T}}_{BC})\overline{\mathcal{T}}_{BC}^n\| \leq c_l \max_{t,s \in \Omega} |E_n(t, s)|,$$

where c_l is a constant and

$$E_n(t, s) := \int_{\Omega} K_{BC}(t, v) K_{BC}(v, s) dv - \sum_{j=1}^n \alpha_j K_{BC}(t, t_j) K_{BC}(t_j, s)$$

Since the kernel functions under consideration are piecewise constant, the quadrature rule is exact, and hence, $E_n(t, s) = 0$.

The remaining terms in (7.4) are $\|(I - \overline{\mathcal{T}}_{BC})^{-1}\|$ and $\|(\overline{\mathcal{T}}_{BC}^n - \overline{\mathcal{T}}_{BC})\bar{b}\|$. The term $\|(\overline{\mathcal{T}}_{BC}^n - \overline{\mathcal{T}}_{BC})\bar{b}\|$ is the quadrature error in the $L^2(\Omega)$ -norm. We connect it to the $L^\infty(\Omega)$ -norm by using the well-known embedding

$$L^\infty(\Omega) \hookrightarrow L^2(\Omega).$$

Hence,

$$\|(\overline{\mathcal{T}}_{BC}^n - \overline{\mathcal{T}}_{BC})\bar{b}\| \leq |\Omega|^{1/2} \|(\overline{\mathcal{T}}_{BC}^n - \overline{\mathcal{T}}_{BC})\bar{b}\|_\infty. \tag{7.5}$$

We can quantify the error with the $L^\infty(\Omega)$ -norm

$$\|(\overline{\mathcal{T}}_{BC}^n - \overline{\mathcal{T}}_{BC})\bar{b}\|_\infty = \frac{2^3 h^2}{12} \max_{x \in \Omega} |\bar{b}''(x)|. \tag{7.6}$$

Consequently, combining (7.5) and (7.6), we obtain

$$\|(\overline{\mathcal{T}}_{BC}^n - \overline{\mathcal{T}}_{BC})\bar{b}\| = \mathcal{O}(h^2).$$

To the best of the authors' knowledge, the term $\|(I - \overline{\mathcal{T}}_{BC})^{-1}\|$ can be quantified only by resorting to a discretized form. However, we have an advantage, namely, we have the bound (7.3) at our disposal. Putting all pieces together, we arrive at the error bound

$$\|u - u_n\| = \mathcal{O}(h^2 \delta^{-2}).$$

Table 7.1
Relative errors in L^2 -norm for varying h when $\delta = 2^{-4}$.

	\mathcal{M}_a	Ratio \mathcal{M}_a	\mathcal{M}_D	Ratio \mathcal{M}_D
$h = 2^{-4}$	0.333655	...	0.027641	...
$h = 2^{-5}$	0.111183	3.00	0.009184	3.00
$h = 2^{-6}$	0.030319	3.66	0.002502	3.64
$h = 2^{-7}$	0.007756	3.93	0.000640	3.90
$h = 2^{-8}$	0.001950	3.97	0.000161	3.97
$h = 2^{-9}$	0.000488	3.99	0.000040	4.02

Table 7.2
Relative errors in L^2 -norm for varying δ when $h = 2^{-5}$.

	\mathcal{M}_a	Ratio \mathcal{M}_a	\mathcal{M}_D	Ratio \mathcal{M}_D
$\delta = 2^{-5}$	0.333414	...	0.027506	...
$\delta = 2^{-4}$	0.111183	2.99	0.009184	2.99
$\delta = 2^{-3}$	0.030367	3.66	0.002521	3.64
$\delta = 2^{-2}$	0.007814	3.88	0.000662	3.81

Table 8.1
Condition number of the periodic operator \mathcal{M}_p .

	$\kappa_e(\mathcal{M}_p)$	$\frac{7.303}{\pi^2} \delta^{-2}$	$\kappa_e(A_p^s)$	$\kappa_e(A_p^s)$ rate
$\delta = 2^{-1}$	3.3359	2.9596	3.3358	–
$\delta = 2^{-2}$	12.1609	11.8384	12.1582	3.64
$\delta = 2^{-3}$	47.5941	47.3536	47.5588	3.91
$\delta = 2^{-4}$	190.1750	189.4144	189.2012	3.97
$\delta = 2^{-5}$	760.7300	757.6576	748.6265	3.96

7.2. Numerical tests verifying the error bound

We report the relative error in $L^2(\Omega)$ for varying values of δ when h is fixed and for varying values h when δ is fixed. We choose the functions $u = \cos(\pi x/2)$ and $u = \sin(x)$ for the antiperiodic and Dirichlet problem, respectively, as the exact solution. We compute the right hand side function b according to given exact solutions. We report the error in Tables 7.1 and 7.2. We observe that the convergence rates are in agreement with our theoretical result.

8. Numerical experiments

For each BC considered, we compare the condition number of the analytic operator \mathcal{M}_{BC} against the discretized operator A_{BC}^s in the form of a symmetric system matrix. This reduces the condition number of the discretized operator to the ratio of the maximum and minimum eigenvalues.

We show the quantifications in Tables 8.1, 8.2, 8.3, and 8.4 for the periodic, antiperiodic, Neumann, and Dirichlet BC, respectively. We use varying values of δ ; $\delta = 2^{-j}$, $j = 1, \dots, 5$. We report the condition number values as a function of the δ values.

We know the eigenvalues λ_{\min}^p and λ_{\min}^a exactly; see (3.8) and (3.14). In fact, for fixed δ , we can also compute the maximal eigenvalue exactly. Due to the decay of the $\text{sinc}(x)$ function, it is sufficient to check only a certain number of k values to find out λ_{\max}^p and λ_{\max}^a . From (2.8), (2.9), and (4.8), we report the exact value $\kappa(\mathcal{M}_{BC})$ for fixed δ and report this in the first column in the related tables.

We report the condition number of the matrices A_p^s , A_a^s , A_N^s , and A_D^s (the third column in the related tables) and these figures are computed with the value of $h = 2^{-9}$. In the last column, we report the growth rate of $\kappa(A_{BC}^s)$ (the fourth column in the related tables) with decreasing δ and clearly see the δ^{-2} behavior with varying δ .

For the case of periodic BC, from (3.11) and (3.12), we know that the coefficient of δ^{-2} lies in interval of $(\frac{6}{\pi^2}, \frac{24}{\pi^2})$. We want to identify this coefficient approximately. Using the improved upper bound we found for (3.9), which is approximately 2.434δ , we obtain an improved approximate coefficient by employing a perturbation expansion of $\frac{2.434 \delta}{2\delta - 2 \frac{\sin(\pi \delta)}{\pi}}$. We conclude that the coefficient is approximately $\frac{7.303}{\pi^2} \delta^{-2}$ and report it (the second column in the related tables) in Table 8.1. In the case of antiperiodic BC, from (3.17) and (3.18), we know that the coefficient of δ^{-2} lies in interval of $(\frac{24}{\pi^2}, \frac{96}{\pi^2})$. In the same way, we conclude that the coefficient is approximately $\frac{29.212}{\pi^2} \delta^{-2}$ and report it in Table 8.2.

For all BC, we see that the condition number of the analytic operator \mathcal{M}_{BC} and its discretized counterpart A_{BC}^s are in good agreement. The condition number clearly depends only on δ and behaves like δ^{-2} .

In Table 8.5, we report the quantification of the condition number of the matrices for different values of h when $\delta = 2^{-2}$. In the last column where we indicate $h \rightarrow 0$, we report the exact value $\kappa(\mathcal{M}_{BC})$ for the choice of $\delta = 2^{-2}$. We observe that

Table 8.2
Condition number of the antiperiodic operator \mathcal{M}_a .

	$\kappa(\mathcal{M}_a)$	$\frac{29.212}{\pi^2} \delta^{-2}$	$\kappa(A_a^s)$	$\kappa(A_a^s)$ rate
$\delta = 2^{-1}$	11.8384	11.8392	11.8376	–
$\delta = 2^{-2}$	47.6029	47.3568	47.5854	4.02
$\delta = 2^{-3}$	190.1843	189.4272	189.6458	3.99
$\delta = 2^{-4}$	760.3800	757.7088	755.3921	3.98
$\delta = 2^{-5}$	3042.8800	3030.8352	2993.6655	3.96

Table 8.3
Condition number of the Neumann operator \mathcal{M}_N .

	$\kappa_e(\mathcal{M}_N)$	$\frac{29.212}{\pi^2} \delta^{-2}$	$\kappa_e(A_N^s)$	$\kappa_e(A_N^s)$ rate
$\delta = 2^{-1}$	12.1610	11.8392	12.2061	–
$\delta = 2^{-2}$	47.6029	47.3568	47.7478	3.91
$\delta = 2^{-3}$	190.1843	189.4272	190.2889	3.99
$\delta = 2^{-4}$	760.7000	757.7088	758.3742	3.99
$\delta = 2^{-5}$	3042.9200	3030.8352	3004.8940	3.96

Table 8.4
Condition number of the Dirichlet operator \mathcal{M}_D .

	$\kappa(\mathcal{M}_D)$	$\frac{29.212}{\pi^2} \delta^{-2}$	$\kappa(A_D^s)$	$\kappa(A_D^s)$ rate
$\delta = 2^{-1}$	12.1610	11.8392	12.1599	–
$\delta = 2^{-2}$	47.6029	47.3568	47.5854	3.91
$\delta = 2^{-3}$	190.1843	189.4272	189.6457	3.99
$\delta = 2^{-4}$	760.7000	757.7088	755.7062	3.98
$\delta = 2^{-5}$	3042.9200	3030.8352	2993.6655	3.96

Table 8.5
Condition number for various h when $\delta = 2^{-2}$.

	$h = \frac{\delta}{2}$	$h = \frac{\delta}{4}$	$h = \frac{\delta}{8}$	$h = \frac{\delta}{16}$	$h = \frac{\delta}{32}$	$h = \frac{\delta}{64}$	$h \rightarrow 0$
$\kappa_e(A_p^s)$	6.8284	10.0474	11.5724	12.0114	12.1231	12.1511	12.1609
$\kappa(A_a^s)$	25.2741	39.2302	45.3704	47.0287	47.4523	47.5587	47.6029
$\kappa_e(A_N^s)$	32.1634	43.8623	47.9481	48.3441	48.1095	47.8864	47.6029
$\kappa(A_D^s)$	26.2741	39.2302	45.3704	47.0287	47.4523	47.5587	47.6029

of $\kappa(A_{BC}^s)$ approaches to $\kappa(\mathcal{M}_{BC})$ as $h \rightarrow 0$. In addition, when $4h \leq \delta$, there is a mild dependence of $\kappa(A_{BC}^s)$ on h and but the figures are getting closer to $\kappa(\mathcal{M}_{BC})$ as $h \rightarrow 0$.

9. Comparison to the original peridynamics operator

We are in a position to make comparison to sharp bounds given in [8]. We used the discretized form of operator of \mathcal{L}_{orig}^h , with nonlocal homogeneous Dirichlet BC. Linear and constant finite element discretizations were used. The sharp lower bound for $\lambda_{\min}(\mathcal{L}_{orig}^h)$ was more demanding than the upper one. We had to exploit sophisticated analysis to find the sharp lower bound. Namely, the nonlocal characterization of Sobolev spaces [28,29] was used to obtain the following bound.

$$\alpha \delta^3 h \leq \lambda_{\min}(\mathcal{L}_{orig}^h). \tag{9.1}$$

For the upper bound, a special function was used together with a Rayleigh quotient argument and we obtained

$$\lambda_{\min}(\mathcal{L}_{orig}^h) \leq \bar{\alpha} \delta^3 h. \tag{9.2}$$

On the other hand, the sharp upper bound for $\lambda_{\max}(\mathcal{L}_{orig}^h)$ was more demanding than the lower one. We had to find out explicit expressions of the stiffness matrix entries. Then, we used an application of the Gerschgorin circle theorem. Assuming $3h \leq \delta$, we obtained the following bound.

$$\lambda_{\max}(\mathcal{L}_{orig}^h) \leq \bar{\beta} (5\delta h - 6h^2). \tag{9.3}$$

For the lower bound, a special function was used together with a Rayleigh quotient argument and we obtained the same lower bound quantification of

$$\bar{\beta} (5\delta h - 6h^2) \leq \lambda_{\max}(\mathcal{L}_{orig}^h). \tag{9.4}$$

Here the constants $\underline{\alpha}$, $\bar{\alpha}$, β , and $\bar{\beta}$ are all absolute constants, meaning that they do not have dependence on δ and h . Furthermore, by using numerical linear algebra techniques related to characterization of the minimal eigenvalue of Toeplitz matrices [30,31], we identified an asymptotic statement regarding the constant $\underline{\alpha}$. More precisely, as $h \rightarrow 0$, we had

$$\underline{\alpha} \rightarrow \frac{3\pi^2}{2}. \tag{9.5}$$

Now, we state our bounds in this paper from a different perspective. We want to translate the bounds for the condition number into bounds for the extremal eigenvalues. For λ_{\max}^p and λ_{\max}^a , we already have (3.9) and (3.15), respectively. Combining (3.9) with (3.13) and (3.15) with (3.19), we arrive at the following bounds.

$$\begin{aligned} \frac{\pi^2}{12} \delta^3 &< \lambda_{\min,2}^p &< \frac{\pi^2}{2} \delta^3 \\ \frac{\pi^2}{48} \delta^3 &< \lambda_{\min}^a, \lambda_{\min,2}^N, \lambda_{\min}^D &< \frac{\pi^2}{8} \delta^3. \end{aligned}$$

Note that the factor π^2 appears in (9.5). The same factor appears in all minimal eigenvalue bounds for the analytic operator. This can be interpreted as indication that the operator $\mathcal{L}_{\text{orig}}^h$ is close to \mathcal{L} when h is small.

10. Conclusion

We explicitly know the eigenvalues of the novel operators under consideration. This brings a major advantage in terms of conditioning analysis. We can determine the exact expression of the condition number in terms of the nonlocality parameter δ . The conditioning analysis boils down to finding sharp bounds for that expression.

In our previous paper [8], we studied a nonlocal operator, the original PD governing operator, which uses nonlocal BC. Since we did not have access to the eigenvalues of that operator, we had to utilize a discretized form. In this paper, for conditioning analysis, we have the ability to work directly with the operator, not its discretized form. Hence, our analysis is easily accessible. From conditioning point view, direct access to eigenvalues provides a better understanding of the role of δ in nonlocal operators. We also proved an error bound with δ and h quantification as follows.

$$\|u - u_n\| = \mathcal{O}(h^2 \delta^{-2}).$$

In [8], combining (9.1), (9.2), (9.3), and (9.4) we arrived at the following sharp bound.

$$\underline{\gamma} (5\delta^{-2} - 6\delta^{-3}h) \leq \kappa(\mathcal{L}_{\text{orig}}^h) \leq \bar{\gamma} (5\delta^{-2} - 6\delta^{-3}h), \tag{10.1}$$

where $\underline{\gamma}$ and $\bar{\gamma}$ are constants independent of δ and h . We can see how the operators $\mathcal{L}_{\text{orig}}^h$ and \mathcal{M}_D are related. As $h \rightarrow 0$, the condition number bounds of $\mathcal{L}_{\text{orig}}^h$ recover that of the operator \mathcal{M}_D , as well as the other operators \mathcal{M}_p , \mathcal{M}_a , and \mathcal{M}_N . The condition numbers of all the considered operators exhibit the same δ^{-2} behavior. Hence, from the conditioning point of view, we conclude that the modifications made to the operator $\mathcal{L}_{\text{orig}}$ to obtain the novel operators are minor.

In [8], we proved a mild dependence on h in $\kappa(\mathcal{L}_{\text{orig}}^h)$ in (10.1) with the additional $\delta^{-3}h$ term. The numerical experiments indicate that there is a also dependence of the condition number of the discretized \mathcal{M}_{BC} operator. This dependence is mild and we observe that $\kappa(A_{BC}^s)$ approaches to $\kappa(\mathcal{M}_{BC})$ as $h \rightarrow 0$.

There is an interesting similarity between the ill-conditioning of the Laplace operator Δ_{BC}^h and that of the nonlocal operator \mathcal{M}_{BC} , i.e., $\kappa(\Delta_{BC}^h) = \mathcal{O}(h^{-2})$ and $\kappa(\mathcal{M}_{BC}) = \mathcal{O}(\delta^{-2})$, respectively. We hope that this observation sheds light on the role of δ in nonlocal problems. For future research, we plan to construct preconditioners to address the ill-conditioning indicated by the δ^{-2} bounds.

Acknowledgments

Burak Aksoylu was supported in part by the European Commission Marie Curie Career Integration 293978 grant and the Scientific and Technological Research Council of Turkey (TÜBİTAK) MFAG 115F473 grant. Portions of this work was also sponsored by ORISE contract 1120-1120-99.

Appendix. Proofs of related bounds

We give the proof of Lemma 3.2.

Proof. (Periodic-lower Bound) The inequality (3.11) is equivalent to proving

$$\frac{6}{x^2} < \frac{1}{1 - \text{sinc}(x)},$$

for $x = \delta\pi$ with $0 < x < \pi$. Hence, we aim to show that

$$0 < f(x) = x^3 - 6x + 6 \sin(x).$$

Since

$$\lim_{x \rightarrow 0} f(x) = 0,$$

proving that $f(x) > 0$ follows from showing that $f(x)$ is strictly increasing. Namely,

$$0 < f'(x) = 3x^2 - 6 + 6 \cos(x).$$

Hence, we need to consider the second and third derivatives of $f(x)$ given as

$$f''(x) = 6x - 6 \sin(x), \quad f^{(3)}(x) = 6(1 - \cos(x)).$$

We also have

$$\lim_{x \rightarrow 0} f'(x) = \lim_{x \rightarrow 0} f''(x) = \lim_{x \rightarrow 0} f^{(3)}(x) = 0.$$

It is clear that $f^{(3)}(x) > 0$. This implies that $f''(x)$ is strictly increasing and from the limit value of $f''(x)$ at $x = 0$, $f''(x) > 0$. Similarly, this implies $f'(x)$ is strictly increasing and from the limit value of $f'(x)$ at $x = 0$, $f'(x) > 0$.

(Periodic-upper bound) The inequality (3.12) is equivalent to proving

$$\frac{3/2}{1 - \operatorname{sinc}(x)} < \frac{24}{x^2},$$

for $x = \delta\pi$ with $0 < x < \pi$. Hence, we aim to show that

$$0 < f(x) = -3x^3 + 48x - 48 \sin(x).$$

Since

$$\lim_{x \rightarrow 0} f(x) = 0,$$

proving that $f(x) > 0$ follows from showing that $f(x)$ is strictly increasing. Namely,

$$0 < f'(x) = -9x^2 + 48 - 48 \cos(x).$$

Hence, we need to consider the second derivative of $f(x)$ given as

$$f''(x) = -18x + 48 \sin(x).$$

We also have

$$\lim_{x \rightarrow 0} f''(x) = 0.$$

By the roots of $f''(x)$, we immediately see that

$$\operatorname{sinc}(x) = \frac{3}{8}. \tag{A.1}$$

The function $\operatorname{sinc}(x)$ is one-to-one for $0 < x < \pi$ and $\frac{3}{8}$ is in the range of the function. Hence, Eq. (A.1) has only one solution. So, $f''(x)$ has only one root and denote it by x^* . Since

$$\lim_{x \rightarrow \pi} f''(x) = -18\pi < 0,$$

$f''(x) > 0$ for $0 < x < x^*$ and $f''(x) < 0$ for $x^* < x < \pi$. Combining the above calculations, the function $f''(x)$ leads to the fact that $f'(x)$ has only one critical point at $x = x^*$ and $f'(x)$ is increasing for $0 < x < x^*$ and decreasing for $x^* < x < \pi$. Since

$$\lim_{x \rightarrow 0} f'(x) = 0, \quad \lim_{x \rightarrow \pi} f'(x) = 96 - 9\pi^2 > 0,$$

finally, we arrive at $f'(x) > 0$ for $0 < x < \pi$. \square

We give the proof of Lemma 3.3.

Proof. (Antiperiodic-lower Bound) The inequality (3.17) is equivalent to proving

$$\frac{6}{x^2} < \frac{1}{1 - \operatorname{sinc}(x)},$$

for $x = \frac{\delta\pi}{2}$ with $0 < x < \frac{\pi}{2}$, which has already been proved in Lemma 3.2 for $0 < x < \pi$.

(Antiperiodic-upper bound) The inequality (3.18) is equivalent to proving

$$\frac{3/2}{1 - \operatorname{sinc}(x)} < \frac{24}{x^2},$$

for $x = \frac{\delta\pi}{2}$ with $0 < x < \frac{\pi}{2}$, which has already been proved in Lemma 3.2 for $0 < x < \pi$. \square

References

- [1] S. Silling, Reformulation of elasticity theory for discontinuities and long-range forces, *J. Mech. Phys. Solids* 48 (2000) 175–209.
- [2] F. Andreu-Vaillio, J.M. Mazón, J.D. Rossi, J. Toledo-Melero, Nonlocal Diffusion Problems, in: *Mathematical Surveys and Monographs*, vol. 165, American Mathematical Society and Real Sociedad Matematica Espanola, 2010.
- [3] Q. Du, M. Gunzburger, R.B. Lehoucq, K. Zhou, Analysis and approximation of nonlocal diffusion problems with volume constraints, *SIAM Rev.* 54 (2012) 667–696.
- [4] P. Seleson, M. Gunzburger, M.L. Parks, Interface problems in nonlocal diffusion and sharp transitions between local and nonlocal domains, *Comput. Methods Appl. Mech. Eng.* 266 (2013) 185–204.
- [5] B. Aksoylu, T. Mengesha, Results on nonlocal boundary value problems, *Numer. Funct. Anal. Optim.* 31 (12) (2010) 1301–1317.
- [6] B. Aksoylu, M.L. Parks, Variational theory and domain decomposition for nonlocal problems, *Appl. Math. Comput.* 217 (2011) 6498–6515. <http://dx.doi.org/10.1016/j.amc.2011.01.027>.
- [7] K. Zhou, Q. Du, Mathematical and numerical analysis of linear peridynamic models with nonlocal boundary conditions, *SIAM J. Numer. Anal.* 48 (2010) 1759–1780.
- [8] B. Aksoylu, Z. Unlu, Conditioning analysis of nonlocal integral operators in fractional Sobolev spaces, *SIAM J. Numer. Anal.* 52 (2) (2014) 653–677.
- [9] H.R. Beyer, B. Aksoylu, F. Celiker, On a class of nonlocal wave equations from applications, *J. Math. Phys.* 57 (6) (2016) 062902. <http://dx.doi.org/10.1063/1.4953252>. EId: 062902.
- [10] B. Aksoylu, H.R. Beyer, F. Celiker, Application and implementation of incorporating local boundary conditions into nonlocal problems, *Numer. Funct. Anal. Optim.* 38 (9) (2017) 1077–1114. <http://dx.doi.org/10.1080/01630563.2017.1320674>.
- [11] B. Aksoylu, H.R. Beyer, F. Celiker, Theoretical foundations of incorporating local boundary conditions into nonlocal problems, *Rep. Math. Phys.* 40 (1) (2017) 39–71. [http://dx.doi.org/10.1016/S0034-4877\(17\)30061-7](http://dx.doi.org/10.1016/S0034-4877(17)30061-7).
- [12] B. Aksoylu, F. Celiker, Comparison of nonlocal operators utilizing perturbation analysis, in: B. Karasözen, M. Manguoğlu, M. Tezer-Sezgin M., S. Göktepe, Ö. Uğur (Eds.), *Numerical Mathematics and Advanced Applications*, ENUMATH 2015, in: *Lecture Notes in Computational Science and Engineering*, vol. 112, Springer, 2016, pp. 589–606. http://dx.doi.org/10.1007/978-3-319-39929-4_57.
- [13] B. Aksoylu, F. Celiker, Nonlocal problems with local Dirichlet and Neumann boundary conditions, *J. Mech. Mater. Struct.* 12 (4) (2017) 425–437. <http://dx.doi.org/10.2140/jomms.2017.12.425>.
- [14] B. Aksoylu, F. Celiker, O. Kilicer, Nonlocal problems with local boundary conditions in higher dimensions. (submitted for publication).
- [15] B. Aksoylu, F. Celiker, O. Kilicer, Nonlocal problems with local boundary conditions: An overview, in: G.Z. Voyiadjis (Ed.), *Handbook on Nonlocal Continuum Mechanics for Materials and Structures*, Springer International Publishing, Cham, 2017. http://dx.doi.org/10.1007/978-3-319-22977-5_34-1 (in press).
- [16] E. Madenci, E. Oterkus, *Peridynamic Theory and Its Applications*, Springer, New York Heidelberg Dordrecht London, 2014. <http://dx.doi.org/10.1007/978-1-4614-8465-3>.
- [17] B. Kilic, *Peridynamic Theory for Progressive Failure Prediction in Homogeneous and Heterogeneous Materials* (Ph.D. thesis), Department of Aerospace and Mechanical Engineering, University of Arizona, Tucson, AZ, 2008.
- [18] J.A. Mitchell, S.A. Silling, D.J. Littlewood, A position-aware linear solid constitutive model for peridynamics, *J. Mech. Mater. Struct.* 10 (5) (2015) 539–557.
- [19] G. Gilboa, S. Osher, Nonlocal operators with applications to image processing, *Multisc. Model Simul.* 7 (3) (2008) 1005–1028.
- [20] Q. Du, R. Lipton, Peridynamics, fracture, and nonlocal continuum models, *SIAM News* 47 (3) (2014).
- [21] S. Silling, R.B. Lehoucq, Peridynamic theory of solid mechanics, *Adv. Appl. Mech.* 44 (2010) 73–168.
- [22] X. Tian, Q. Du, Analysis and comparison of different approximations to nonlocal diffusion and linear peridynamic equations, *SIAM J. Numer. Anal.* 51 (6) (2013) 3458–3482.
- [23] T. Mengesha, Q. Du, Analysis of a scalar peridynamic model for sign changing kernel, *Disc. Cont. Dyn. Sys. B* 18 (2013) 1415–1437.
- [24] P. Seleson, M.L. Parks, On the role of the influence function in the peridynamic theory, *Int. J. Multisc. Comput. Eng.* 9 (6) (2011) 689–706.
- [25] K. Atkinson, W. Han, *Theoretical Numerical Analysis*, Springer Verlag, New York, Berlin, Heidelberg, 2009.
- [26] R. Kress, *Linear Integral Equations*, Springer-Verlag, Berlin, Heidelberg, 1989.
- [27] K. Atkinson, *The Numerical Solution of Integral Equations of the Second Kind*, Cambridge University Press, Cambridge, 1997.
- [28] J. Bourgain, H. Brézis, P. Mironescu, Another look at Sobolev spaces, in: J.L. Menaldi, E. Rofman, A. Sulem (Eds.), *Optimal Control and Partial Differential Equations, a Volume in Honour of a. Benssoussan's 60th Birthday*, 2001, pp. 439–455.
- [29] A.C. Ponce, An estimate in the spirit of Poincaré's inequality, *J. Eur. Math. Soc.* 6 (1) (2004) 1–15.
- [30] A. Böttcher, H. Widom, From Toeplitz Eigenvalues through Green's Kernels to Higher-order Wirtinger-Sobolev Inequalities, *Oper. Theory Adv. Appl.* 171 (2007) 73–87.
- [31] M. Kac, W.L. Murdock, G. Szegő, On the eigenvalues of certain hermitian forms, *J. Rational Mech. Anal.* 2 (1953) 767–800.